UNDERSTANDING GENETIC REGULATION OF UV-B RESPONSES IN *ARABIDOPSIS THALIANA*

Stephanie J. Smith

A Thesis Submitted to the
University of North Carolina Wilmington in Partial Fulfillment
of the Requirements for the Degree of
Master of Science

Department of Biology and Marine Biology

University of North Carolina Wilmington

2008

Approved by

Advisory Committee

Ann Stapleton

Ann Pabst

Ann Stapleton
Chair

Accepted by

Robert D. Roer

Digitally signed by Robert D. Roer
DN: cn=Robert D. Roer, o=UNCW, ou=Dean of the Graduate School & Research, email=roer@uncw.edu, c=US
Date: 2008.05.21 11:15:57 -04'00'

Dean, Graduate School

TABLE OF CONTENTS

ABSTRACT

Light plays a major signaling role in plant growth and development, which directly involves plant photoreceptors. UV-B radiation (280-320nm) is also an integral component of sunlight that may cause damage to macromolecules or activate adaptive responses. Using genes known to be UV-inducible from previous microarray experiments, I measured gene expression after UV-B exposure using real-time PCR in wild-type *Arabidopsis* seedlings, and then compared wild-type gene expression to expression in a putative UV-B photoreceptor mutant. I also monitored the effect of UV-B on growth, which was measured by leaf rosette diameter. In two experimental settings, there were significant differences between treatments (Mylar and cellulose diacetate), genotypes (mutant and wild-type), and their interaction. Based on these results, I conclude that the candidate gene fits the phenotype of a UV-B photoreceptor and confers increased growth in the greenhouse when the photoreceptor is present in plants exposed to UV-B radiation.

ACKNOWLEDGEMENTS

First, I would like to acknowledge the National Science Foundation (NSF) for funding my research during my graduate career. I would like to express my appreciation to my advisor, Dr. Ann Stapleton, for her training, guidance and wisdom throughout this entire process, all of which were essential to my success. I would also like to thank my thesis committee members, Dr. Ann Pabst and Dr. Alison Taylor, for their expert advice and support. I would like to thank Dr. Bongkeun Song for his patience and support with my experiments at the Center for Marine Science (CMS). I also want to thank the greenhouse manager, Ms. Jennifer Messer, for diligent care of my plants during experimentation. Special thanks to Dr. Susan Simmons for her expertise in statistical analysis. Lastly, I want to thank the graduate school at UNCW for giving me a chance to finish my master's degree.

LIST OF TABLES

LIST OF FIGURES

INTRODUCTION

Light plays a major signaling role in plant growth and development. Photoreceptors are light-sensitive proteins involved in the sensing and co-ordination of responses to light in a variety of organisms (Briggs and Olney, 2001). These photoreceptors include well-studied systems involved in plant responses to blue light (cryptochromes and phototropins) and red light (phytochrome system) (Taiz and Zeiger, 1998). Phototropins mediate phototropism responses in higher plants, such as stomatal opening, and are activated in response to blue light (DeBlasio et al., 2005). The phytochrome family of photoreceptors is specific to red light (RL) and far-red (FR) light perception, whereas the cryptochrome family specifically perceives blue light (BL) and UV-A light (Quail, 2002). Although red light, mediated through phytochrome, can induce phototropic responses under special circumstances (Parker et al., 1989), it seems probable that specific BL photoreceptors play an important role in most light-responsive growth and movement (Hashimoto, 1994). Phytochromes that absorb red/far-red light and cryptochromes that sense UV-A/blue light together regulate photomorphogenetic processes. These processes include deetiolation (stem elongation, leaf expansion etc.), vegetative growth, flowering induction, and circadian rhythms (Smith, 2000; Lin, 2002; Morelli and Ruberti, 2002; Wang and Deng, 2002). In *Arabidopsis thaliana*, at least 10 photoreceptors, including five phytochromes (phyA through phyE), three cryptochromes (cry1, cry2, and cry3), and two phototropins (phot1 and phot2), have been identified (*Arabidopsis* Genome Initiative, 2000).

Over the past decades, rising UV-B fluence (radiation intensity) rates at the earth's surface caused by stratospheric ozone depletion has attracted researchers to want

to better understand UV-B light signal perception and transduction (Suesslin and Frohnmeyer, 2003). UV-B tolerance mechanisms are commonly studied because they are directly relevant to changes in terrestrial UV-B fluence. UV-B radiation causes a multitude of responses that are defined as low- and high-fluence responses similar to phytochrome responses (Kim et al., 1998). "High-fluence" response pathways, generally include DNA damage signaling, and "low-fluence" pathways are mediated through one or more UV-B photoreceptor proteins (Frohnmeyer and Staiger, 2003). (Fig. 1)

Although UV-B radiation (280-320 nm) is an important component of sunlight, significant increases above natural levels are harmful to plants. High fluence UV-B can cause damage to vital cellular molecules, such as DNA and generative reactive oxygen species (Frohnmeyer and Staiger, 2003). Plants have the ability to partly protect themselves from UV with various internal response methods. For most plants only a small proportion of the UV-B radiation striking a leaf penetrates very far into the inner tissues. Also, when exposed to an enhanced UV-B level, many species of plants can increase the UV-absorbing pigments in their tissues. Other adaptations to this stress include increased thickness of leaves, which reduces the proportion of inner tissues exposed to UV-B radiation (UNEP, 1998).

One method that can be used to identify proteins with known UV photoreceptor characteristics in the *Arabidopsis* genome is a bioinformatics approach. This approach was used to identify proteins with known photoreceptor characteristics in the *Arabidopsis* genome (Stapleton, 2006). According to Stapleton (personal communication), the final list of identified proteins had no known function and no PubMed citation, but good annotation and EST (Expressed-Sequence-Tags) coverage. ESTs are short, unedited,

single pass sequence reads derived from randomly selected complementary DNA (cDNA) libraries (Nagaraj et al., 2007). The top-ranked final candidate gene containing PAC/PAS domains, but no kinase domain, was gene ID At2g02710. PAS (Per-ARNT-Sim) domains are frequently followed by a 40- to 50-amino acid PAC motif, is likely to contribute to PAS structural domain (Ponting and Aravind, 1997). PAS/PAC domains are proposed to form a single structural element (Taylor and Zhulin, 1999) and thus are referred to as PAS/PAC domains (Catlett et al., 2003).

The best-characterized low fluence UV-B-mediated responses in *Arabidopsis thaliana* are the inhibition of hypocotyl growth in seedlings, the biosynthesis of UV-absorptive secondary metabolites such as flavonoids or sinnapate esters, and the stimulation of related gene expression changes (Boccalandro et al., 2001; Christie and Jenkins, 1996; Kim et al., 1998; Landry et al., 1995; Li et al., 1993). Brown et al. (2005) characterized an *Arabidopsis* gene, UV RESISTANCE LOCUS 8 (*UVR8*). They tested whether the mutants in the gene responded to UV-B, whether the gene was apart of a cascade of genes involved in a UV-B signaling pathway, and whether the proposed pathway of which *UVR8* gene is a part, plays a role in protecting the plant from UV. Their results show that *UVR8* is a UV-B-specific signal transduction component that plays an important role in mediating plant responses to UV. In particular, *UVR8* works in combination with the protective gene expression responses (enabling plants to protect themselves from harmful sunlight). Thus, *UVR8* defines a key light-signaling pathway in plants (Brown et al., 2005). Genes identified that play a role in signaling pathways can also play a role in other biological plant processes such as flavonoid biosynthesis.

In addition to flavonoid biosynthesis, which is responsible for the color of flowers and fruits and can function to protect plants from UV, and plant defense mechanisms, two morphogenic responses to UV-B have been identified in *Arabidopsis*, which include cotyledon opening and the inhibition of hypocotyl elongation (Suesslin and Frohnmeyer, 2003). Suesslin and Frohnmeyer (2003) isolated UV-B hypersensitive mutants with reduced tolerance to UV-stress to investigate UV-B mediated responses in *Arabidopsis*. A UV-B light sensitive protein (*ULI3*) was identified, which was found to be a specific component involved in UV-B-mediated signal transduction of protection mechanisms and various morphological responses to UV-B light (Suesslin and Frohnmeyer, 2003). *ULI* mutants are specifically impaired in UV-B-mediated responses and have highly specific signaling function during early developmental stages in *Arabidopsis* (Suesslin and Frohnmeyer, 2003). The physiological features of the *ULI3* mutant resemble those of other *Arabidopsis* mutants that had been isolated due to impaired responses to red, far-red or blue light and later found to be affected either in the function of a specific photoreceptor or in signaling triggered by this photoreceptor (Ahmad and Cashmore, 1993; Cashmore et al., 1999; Nagatani et al., 1993; Reed et al., 1993; Somers et al., 1991.). *ULI3* gene expression was found in all active organs such as flowers and stems but not in roots. Suesslin and Frohnmeyer (2003) places *ULI3* function close to a UV-B photoreceptor in signal transduction, where it might be activated by electron transfer and in turn activate downstream elements of UV-B signaling by membrane attachment, electron transfer, or both. Although experiments examining UV-B signaling responses have shown that proteins encoded by *UVR8* and *ULI3* do not directly absorb UV-B, they

are nevertheless essential components in signaling after photoreception (Ulm and Nagy, 2005).

Boccalandro et al. (2001) determined that cotyledon opening has especially useful features for photoreceptor mutant screens as the hypocotyl shortening-response appears to have both low-fluence and high-fluence components. Their results suggest that the effects of UV-B on cotyledon opening and hypocotyl growth inhibition are mediated through different photosensory mechanisms within the same developmental stage of the *Arabidopsis* seedling. Isolation and characterization of mutants with altered morphogenic responses to UV-B will be necessary to positively identify UV-B receptor systems (Boccalandro et al., 2001). These analyses could lead to the identification of the specific photoreceptors responsible for the inhibition of cotyledon opening.

According to Stapleton (personal communication), to confirm a particular response as photoreceptor-mediated, a few conditions must be met. First, the dose-response curve for the response peaks must be at very low fluence. This will differentiate the responses due to DNA damage, which increases with fluence from the responses due to photoperception and signaling. Second, the response should not be altered by the presence of DNA repair mutations. This will assist in eliminating DNA-damage response pathways. Finally, the response should be UV-B specific in order to focus on one specific response pathway (Stapleton, 2006). The genes and the interactions of the genes involved in the signal transduction pathway are not completely understood. Identification of some genes involved such as *UVR8* and *ULI3* are steps towards better understanding the affects of UV-B and signal transduction pathways involved. Understanding gene expression

regulation as a result of UV-B signaling is key in better understanding signal transduction.

Microarrays are used to analyze the expression of several thousand genes to identify tissue-specific expression patterns and to identify candidate genes for further more detailed analysis (Girke, 2000). Knowing where and when promoters are active and where gene products (RNA and protein) are found can provide important clues to the *in vivo* function of genes. Various methods can be used to analyze gene expression in *Arabidopsis*, such as complementary DNA (cDNA) and oligonuclotide microarrays (Weigel and Glazebrook, 2002).

Brown et al. (2005) examined the expression profiles of UV RESISTANCE LOCUS 8 (*UVR8*) by using whole-genome microarrays in *Arabidopsis*. This work, along with others, set the stage for further investigation of molecular mechanisms enabling plants to cope with increasing levels of UV-B, ultimately leading to a more complete understanding of plants' responses UV-B. The microarray experiments monitored the gene expression profile of UV-B-irradiated seedlings by using high-density oligonucleotide microarrays comprising almost the full *Arabidopsis* genome. Their results provided evidence that UVR8 regulates the expression of various genes that are involved in protecting the plants from damaging UV-B. This pathway does not require known photoreceptors, such as phytochromes, cryptochromes, and phototropins, but involves ELONGATED HYPOCOTYL5 (*HY5*) (Ulm et al., 2004, Brown et al., 2005). *HY5* is a basic domain/leucine zipper (bZIP) transcription factor mediating a number of red and blue light photoreceptor-controlled physiological responses (Osterlund et al., 2000; Chen et al., 2004). *UVR8* is also a key component that assists in the production of

chalcone synthase (*CHS*) expression. Brown et al. (2005) concluded that the *UVR8* pathway plays an important role in plant survival in the natural environment and after exposure to low levels of UV-B. Specifically, *UVR8* regulates the protective gene expression responses that enable plants to survive in response to UV-B.

Some of the light signaling pathways identified are also sensitive to other factors that affect the regulation of gene expression. Recent studies have established a role for reactive oxygen species (ROS) in regulation of gene expression in response to UV-B radiation (Green and Fluhr 1995; Surplus et al. 1998; A.-H Mackerness et al. 1999). Other factors that have been implicated in plant responses to UV-B stress are jasmonic acid (JA), salicylic acid (SA), and ethylene. Mackerness et al. (1999) investigated the role of ROS, JA and ethylene in signal pathways leading to changes in gene expression in *Arabidopsis* in response to UV-B exposure. Their results showed that ROS is also required for the UV-B-induced regulation of PDF1•2 genes, which are defense genes. They also showed that some protection for the plant against UV-B radiation occurs by defense mechanisms which require both JA and ethylene-dependent signaling pathways. Overall, some of the pathways that are involved in response to UV-B exposure indicate that the effects of UV-B on gene expression are unlikely to be due to various damaging factors, such as DNA damage. It is implied that it could be due to UV-B photoreceptor(s) (Macherness et al., 1999).

Fitness is also a factor in *Arabidopsis* that is affected in response to UV-B. UV-B can influence the plant's rate of development and induce morphological responses that may affect fitness. In general, plant fitness is the ability of the plant to reproduce; fitness is often correlated with growth rate. Ganeteg et al. (2004) developed an assay to measure

the fitness of *Arabidopsis* plants under natural conditions by measuring seed production. This method identified whether the photosynthetic light-harvesting complex (LHC) proteins affect the fitness of *Arabidopsis* plants in the field; LHC proteins are responsible for the molecular function of chlorophyll binding. Ganeteg et al. (2004) planted LHC protein deficient plants and their related wild-types. The mutant plants had less seed production. Overall, they concluded that most, and probably all, of the studied proteins have a significant effect on plant performance under natural conditions, which supports the view that each LHC protein is important for plant fitness.

Traw et al. (2007) tested the benefit of systemic acquired resistance (SAR) and jasmonic acid (JA)-mediated defense in an *Arabidopsis* population known to contain pathogenic bacteria. They also tested for direct effects of agrimycin (antibiotic) and salicylic acid (SA) on fitness. Fitness was measured by the amount of shoot dry mass, silique number, and seeds per silique. SAR- and JA-mediated defenses have been shown to suppress the growth of many different kinds of bacteria in the lab and each is associated with the up-regulation of hundreds of genes with known or predicted roles in defense (Schenk et al., 2000). They found that *Arabidopsis thaliana* plants treated with JA received significantly lower insect damage to their siliques, but exhibited no differences in bacterial growth or other measures of fitness relative to controls. Overall, their data suggest a likely role of pathogenic bacteria in the maintenance of SAR, but no jasmonate-dependent resistance in nature (Traw et al., 2007).

The effect of UV on growth in *Arabidopsis thaliana* has not been fully investigated; therefore it is not yet known whether increased UV-B positively or negatively affects plant growth. If the candidate gene, At2g02710, is a UV-B photoreceptor, then I expect

that *Arabidopsis'* UV-B receptors would increase gene expression and growth in the wild-type in laboratory and greenhouse grown plants in response to UV-B.

To test my hypothesis that At2g02710 is a UV-B receptor, I examined whether mutation of this gene resulted in a phenotype supporting the proposed function as a UV-B photoreceptor. To accomplish this goal, two approaches were used. First, I monitored genes known to be UV-inducible from previous microarray experiments. The expression of these genes was determined using real-time PCR in *Arabidopsis* wild-type siblings, compared to the expression in the putative UV-B photoreceptor mutant. Secondly, I tested the candidate gene mutants to see if growth is altered under UV by measuring rosette diameter from leaf tip to tip over a four week time period.

MATERIALS AND METHODS

Planting Arabidopsis Seeds

Seeds were provided by A. Stapleton from the *Arabidopsis* Biological Resource Center (ABRC) (http://www.biosci.ohio-state.edu/~plantbio/Facilities/abrc/abrchome.htm). Seeds with an insertion mutation in the gene of interest (At2g02710), were ordered from the *Arabidopsis* stock center for comparison testing between the mutant and the wild-type. The insertion mutants chosen were named 600 and 6F. The 600 mutant was heterozygous; when selfed, we identified [by Polymerase Chain Reaction (PCR) test], two mutant siblings, which were named 600I and 600A. One wild-type sibling was identified and named 600C. The 6F insertion mutant was homozygous. These plants were crossed to Columbia (Col); a wild-type plant, selfed and 6Fsx was identified by PCR testing. Comparisons were made between the wild-types (Col, 600C, and 6Fsx) and the mutants (600I, 600A, and 6F).

For gene expression measurements the seeds were planted in a water/agar medium with a ½x Muarshige and Skoog Basal Salt mixture (Sigma, St. Louis, MO). The seeds were planted on the media in a 28mm diameter plastic dish with 10-15 seeds per dish. The planted seeds were placed in the refrigerator for about a week. The planted seeds were then exposed to light at room temperature. The light was provided by Phillips 40-watt cool-white and grow-bulb fluorescent bulbs, which allowed the seeds to germinate and to expand their cotyledons.

To measure plant growth, seeds were planted in pots with Metromix soil and allowed to grow until seed production. One seed per pot was planted into wet soil and then gently covered with saran wrap. The seeds were placed in a cold room at 4°C for

approximately 3 days to initiate germination and then were exposed to light at room temperature. The light was provided by cool-white and grow-bulb fluorescent bulbs, which allowed the seeds to germinate and to grow through their full life cycle.

UV Treatments

The seedlings used for the gene expression experiments were placed under UV lamps for thirty minutes with two plastic covers: cellulose diacetate, which allows UV-B to pass through, and Mylar, which is used as a control and does not allow UV-B to pass through. The plants were then provided a one-hour recovery in the growth lights before harvesting for real time-Polymerase Chain Reaction (RT-PCR).

For the growth experiment, the seedlings were given 30 minutes of UV everyday using two plastic covers. In Dobo Hall Room 104, half of the bulbs were covered with Mylar, a Mylar divider was used to separate the potted growth trays, and a cellulose diacetate cover was placed over the other half of the bulbs. The UV was provided by one UV313 bulb that was positioned between two cool-white and grow-bulb fluorescent bulbs.

In the UNCW Kresge greenhouse, the seedlings were also given 30 minutes of UV everyday. The growth apparatus was a large, metal shelf that contained two aluminum tables. The growth trays were on each of the separate aluminum tables approximately two feet off of the ground. On both tables there were two UV313 bulbs in one fixture that hung above the growth trays. One set of UV bulbs were covered with a Mylar plastic cover, while the other set of UV bulbs were covered with a cellulose diacetate cover.

RNA Extraction

After UV treatments and recovery in light, approximately 4-5 seedlings from each dish were harvested into a microfuge tube. Liquid nitrogen was added, the sample was ground to a powder, and Trizol (Invitrogen, Carlsbad, CA) was added. According to manufacturer's instructions, chloroform was added to the Trizol; the mixture was vortexed for 10 seconds and was incubated at room temperature for 5 minutes. The sample was centrifuged at 4°C and the upper phase was pipetted into a new microfuge tube without disturbing the pellet. Isopropanol and 75% ethanol were added to precipitate the RNA and to wash all other solutions from the extracted RNA. After centrifugation ethanol was carefully removed without disturbing the pellet. The remaining RNA sample was left to air-dry for 10 minutes and resuspended in deionized water. The sample was heated to 65°C and vortexed to dissolve the pellet. The RNA sample was stored at -70°C.

Real-time PCR

Primer dilutions were made for each primer with ultrapure water. The primers that were used are specific for known genes, which include actin as a control and putative UV-affected genes, HY5, At5g59820, At5g18470, At4g15480, At2g32020, At2g38940, and At2g32020 (Ulm et al., 2006).

Overall master mixes for each primer were made, which contained 2x SYBR Green QRT-PCR master mix (Stratagene), ultrapure water, RT/RNase block enzyme, and the specific left and right primers for the individual genes. The overall master mixes and the different genomic RNA samples were mixed then amplified using a RT-PCR two-step cycling protocol (Stratagene, La Jolla). Stage 1 includes one cycle of 30 minutes at 50°C, stage 2 includes one cycle of ten minutes at 95°C, and stage 3 includes 40 cycles of

fifteen seconds at 95°C along with one minute at 60°C. A dissociation step was included for verification of the quality of the primers that were being used. The dissociation step is stage 4, which includes one cycle for fifteen seconds at 95°C, one minute at 60°C, and fifteen seconds at 95°C.

For the time course experiment, a total of three replicate samples of Col RNA samples were used with each time course and each treatment. For the gene expression experiments, a total of six replicate samples of each genotype were tested with both treatments in each RT-PCR experiment. Some of the RNA samples resulted in an undetermined Ct value, therefore resulting in a decrease in replicate number. For each separate RT-PCR amplification of the set of eight gene primer pairs, the same six replicate RNA samples were used.

The output from the RT-PCR experiments was summarized as in a threshold cycle (Ct) value. The threshold cycle indicates the fractional cycle number at which the amount of amplified copies reaches a fixed threshold. The Ct values for each primer were divided by the Ct value from the actin primers (i.e. control) for each sample to obtain the "adjusted for actin" Ct values.

Plant Measurements

After two weeks of growth, digital photos were taken of the plants once a week using a Nikon Coolpix 995 digital camera. The camera was manually attached to a camera stand that consisted of a flat, wooden platform that supported the plant growth tray. The growth trays were always placed with the treatment title on the far left, which allowed approximately a two-foot distance from the camera to the plants for every picture. To measure growth, the plant rosette diameter was determined using Image J

(Wayne Rasband, NIH) image processing software. For each image a crop tool was used to specify the area around the plant to enhance the visibility of the leaves, and a linear tool was used to measure the length of the rosette from edge to edge. The same rosette orientation was measured in every digital photo by using manual indicator marks on the first photo taken. The digital photos helped maintain the leaf orientation to ensure the same dimensions were measured. The coefficient of variation of the same measurement made eight times was 1.15%.

Statistical Analysis

Relative Expression Software Tool (REST) was used to compare two treatment groups or conditions (Pfaffl, 2002). The version of REST used allowed me to adjust the actin housekeeping gene amounts per sample tested and determined if the putative UV-inducible genes were up- or down-regulated by UV-B.

Next, a bootstrap permutation method (non-parametric) was used to identify significant differences among genotypes and treatments and to determine if there was a significant interaction between genotypes and treatments. An ANOVA in JMP statistical software (SAS, Inc.) was also used to identify the same significance as the bootstrap permutation. Tukey's HSD and Dunnett's post hoc tests were used to identify which treatment (Mylar or cellulose diacetate), genotype (mutant or wild-type), and interactions were significantly altered in response to UV.

For the growth measurements, the appropriate statistical analysis was a regression, which identified whether there was a significant relationship between the genotype and treatment over time based on their slopes. This was carried out using

GraphPad Prism (GraphPad Software, Inc.), which provides curve fitting and comparison methods.

RESULTS

Time Course

A time course experiment was conducted to assess the effect of increasing the time of UV-B exposure on gene expression. Columbia (wild-type) was used in these experiments. The times of UV-B exposures used were 15 minutes, 30 minutes, and 60 minutes with a one-hour recovery period to allow plants to express genes as a result of the treatment. RT-PCR was used to measure the amount of HY5 gene expression, which was represented by a Ct value. A Ct value is the first cycle in which there is a significant increase in fluorescence above the background noise. The lower the Ct value, the more RNA in the sample, therefore the more gene expression has increased. To adjust for different amounts of RNA in different plants, actin primers were used to measure actin expression and the actin Ct value was divided into the HY5 expression value for each sample. At each time, there was a smaller Ct and thus more expression under cellulose diacetate as compared to Mylar (Fig. 2). The 15 min and the 60 min Mylar had high variance, so the 30 min time course was chosen.

Multiple gene expression comparisons:

Pairwise REST analysis within each genotype

After deciding on a time course, seven known UV-affected genes were chosen from previous microarray experiments to confirm if the genes were altered by UV-B under our exposure conditions. RT-PCR was used to measure the amount of gene expression that occurred among the wild-type and mutant genotypes, with each gene

used. The wild-type genotypes used were Col, 600C, and 6Fsx. The mutant genotypes used were 600I, 6F, and 600A. The genes used include HY5, At5g59820, At5g18470, At4g15480, At3g25250, At2g38940, and At2g32020. Relative Expression Software Tool (REST) was used to determine if these previously identified UV-affected genes were up- or down-regulated by UV-B (Table 2). The consistently regulated genes among the wild-types were At4g15480, At3g25250, and At2g32020. All three of these genes were up-regulated by UV-B; they showed an increase in gene expression in the wild-types. The consistently regulated genes among the mutants were At5g18470, At3g25250, and At2g38940. All three of these genes were down-regulated by UV-B. The gene that was consistently contrasting by UV-B was At3g25250. This gene was up-regulated by UV-B in the wild-type and down-regulated by UV-B in the mutants.

Comparison of expression levels within each genotype

The three genes that appeared to have consistent expression differences in response to UV-B were examined in more detail by graphical comparison. The mutants appeared to have slightly lower expression and thus a higher Ct value under cellulose diacetate when gene At5g18470 was plotted (Fig. 3), although the differences were not large.

When the RT-PCR results for gene At3g25250 were plotted, the mutants appeared to have lower expression under cellulose diacetate, except 6F (Fig. 4). The wild-types had higher expression under cellulose diacetate. These differences between the treatments were not large.

When the RT-PCR results for gene At3g25250 were plotted, the mutants appeared to have lower expression under cellulose diacetate, except 600I (Fig. 5). All of the wild-

types appeared to have higher expression under cellulose diacetate. However, these differences between the treatments were not large. There appeared to be no consistent pattern of expression differences between the mutant and the wild-type *Arabidopsis* plants.

Comparison of expression levels for each genotype by non-parametric analysis

I next compared the effect of UV-B for each gene in each genotype using a statistical test, a non-parametric bootstrap. This analysis was used to identify significant differences among genotypes and treatments, and to determine if there was a significant interaction between genotypes and treatments. Of the seven genes tested, there were no significant differences between the mutant and the wild-type genotypes or the treatments (Table 3). There was a significant interaction detected with gene At3g25250 with a p-value of 0.046 and an indication of an interaction detected with gene At2g32020 with a p-value of 0.108.

Comparison of mutant and wild-type classes in response to UV-B

As there was no consistent difference visible between the three wild-types, I tentatively concluded that the wild-types were correctly identified and grouped all mutants and wild-types together for analysis. An ANOVA indicated that four of the six genes were significantly different in expression level in the mutants, but that these differences were not relevant to the response to UV-B, as the interaction between treatment (either Mylar and cellulose diacetate) and genotype (either mutant and wild-type) was not significant (Table 4).

A Tukey's HSD test indicated that in one of the six genes there was a significant difference between treatments, but these differences were not consistent (Table 5). The

gene that showed a significant difference was At4g15480. The test also indicated that in five of the six genes there was a significant difference between the mutant and the wild-type genotypes. The only gene that did not show a significant difference was the At4g15480 gene. There also appeared to be significant interactions with the genes At3g25250 and At2g32020. However, even though there were significant interactions, these results are inconclusive since there were no differences between treatments in the mutants and wild-types.

A Dunnett's test indicated that for five of the six genes, there was a significant difference in expression level in the mutants when compared to Columbia wild-type (Table 6). The only gene that did not show a significant difference was the At2g38940 gene.

Growth comparison of mutant and wild-type genotypes:

Growth in laboratory conditions:

A linear regression was used to fit a straight line through my data to determine whether the slopes and/or intercepts were significantly different and if their 95% confidence intervals overlap. This analysis indicates whether growth was significantly altered by UV-B over a four-week time period. All of the mutants and the wild-types appear to have better growth with the Mylar treatment (Fig. 6-10). The wild-types with the cellulose diacetate treatment had very little growth (Fig. 6-8). Their 95% confidence intervals do not overlap, which indicates that the slopes and lines are significantly different (Table 7-11).

A global non-linear regression was also used, which fits a family of curves at once with some shared parameters between data sets (Motulsky, 1999). This analysis

indicates whether the interaction of the mutant and the wild-type with both treatments were significantly different over a four-week time period. The mutants and the wild-types appear to have better growth with the Mylar treatment (Fig. 11). According to the mid-point (IC50) values, it confirms that the mutants and the wild-types showed increased growth under the Mylar treatment (Table 12).

Growth in greenhouse conditions

A linear regression was used to fit a straight line through my data to determine whether the slopes/intercepts were significantly different and if their 95% confidence intervals overlap. This analysis indicates whether growth was significantly altered by UV-B over a four-week time period. The wild-types appear to have better growth with the cellulose diacetate treatment, except for 600C, which had better growth with the Mylar treatment (Fig. 12-14). Two of the wild-types, 600C and 6Fsx, had 95% confidence intervals which overlapped, which indicated that the lines are not significantly different (Table 13-15). The mutants appear to have no difference in growth regardless of treatment (Fig. 15-16). Their 95% confidence intervals overlap, which indicates that the lines and the slopes are not significantly different (Table 16-17).

A global non-linear regression was also used, which fits/defines a family of curves at once with some shared parameters between data sets (Motulsky, 1999). This analysis indicates whether the interaction of the mutant and the wild-type with both treatments were significantly different over a four-week time period. The wild-types appear to have less growth with the Mylar treatment (Fig. 17), as they have a larger IC50 value. However, according to the mid-point (IC50) and 95% confidence intervals, there is

no difference in growth between the mutants and the wild-types regardless of treatments (Table 18).

DISCUSSION

UV-B radiation has many direct and indirect effects on plants (Hectors et al., 2007). In *Arabidopsis thaliana*, very little is known about the molecular events, such as gene expression and growth, affected by UV-B. Here I wanted to examine whether or not a candidate gene, At2g02710, fits the phenotype of a UV-B photoreceptor. This gene was chosen using a bioinformatics approach, since the gene had no known function and had not been characterized in detail. Insertion mutants were chosen for comparison testing. Here I show that the gene expression was higher in the wild-type with the selected genes, when compared to the mutants. However, these genes are not significantly altered in expression in response to UV-B under our conditions. UV-B also increased growth in the wild-type in comparison to the mutants in the greenhouse experimental setting. This result suggests that the candidate gene fits the proposed function as a UV-B photoreceptor.

In this research, I first examined a time course of exposure to UV-B. Columbia wild-type plants were exposed to three increasing times of UV-B exposure. As the 15-minute and 60-minute time courses with the Mylar treatment showed high variance, the 30 minute time course was chosen. Hectors et al. (2007) assumed that the UV-B dose rates used in their experiments were too low to activate UV-affected genes, suggesting that a little more UV may be required to activate a larger variety of UV-affected genes. In

contrast, 5-minute UV-B pulses were sufficient to cause growth changes without visible signs of DNA damage in other UV-B experiments (Suesslin and Frohnmeyer, 2003).

Ulm et al. (2004) conducted microarray experiments, which quantitatively assessed changes in response to UV-B radiation in *Arabidopsis*. Seven of the genes they identified were chosen for my study to test the response to UV-B under my UV-B conditions. The genes At3g25250 and At2g32020 were found to have increased gene expression after UV-B exposure, while At2g38940 was down-regulated, although these differences were not significant. Thus my UV-B exposure conditions appear to be different than the cutoff filter conditions used by Ulm et al. (2004).

I next examined whether UV-B affected gene expression of various *Arabidopsis thaliana* wild-types and mutants. The expression of these genotypes was determined using real-time PCR Ct values. Three of the seven genes were found to have consistent expression differences in response to UV-B. Columbia wild-type tended to have more expression of the seven genes overall, which suggests that it is reasonable to compare the mutants to their wild-type siblings instead of just comparing to Columbia.

In general, the mutants had a trend toward lower expression, when compared to the wild-type in response to UV-B. There was no significant interaction effect on these genes, therefore the difference between the mutant and the wild-type is difficult to determine. Overall, gene expression was lower in the mutants when compared to the wild-types with the cellulose diacetate treatment. This may be due to the inactivation of the candidate gene, which therefore alters gene expression. Thus the expression changes observed may not be directly due to UV-B. This observation is consistent with gene

expression studies that have revealed that UV-B activates several genes that also mediate various responses besides protection, such as pathogen resistance (Ulm and Nagy, 2005).

From the non-parametric bootstrap and ANOVA, there appear to be slight differences between the mutant and the wild-type. These differences were seen mainly when the mutants were compared to Col (wild-type), but there was a significant interaction with the At3g25250 gene. The significant interaction was between Col (wild-type) with the cellulose diacetate treatment and the mutants with either treatment.

To identify whether UV-B differentially affects growth, plants were exposed to 30 minutes of UV-B everyday in two different experimental settings. In Dobo room 104, the mutants and wild-types appeared to have better growth with the Mylar treatment when compared to cellulose diacetate, which was not expected. The wild-type and mutant plants appear to be equally responsive to UV-B under these conditions. This suggests that UV-B did not alter growth with any genotype; therefore there is no significant difference between the mutant and wild-type. The inconclusive results may be due to cracks in a growth tray that prevented the Col (wild-type) plants from receiving sufficient water for growth under the cellulose diacetate treatment.

In the greenhouse experimental setting, UV-B increased growth in the wild-type in comparison to the mutant (Fig.12-14). Growth was not altered in the mutant regardless of treatment, which is consistent with my hypothesis. My hypothesis predicted that the insertion mutants with the deficiency in the assumed UV-B responsive photoreceptor, growth should not be altered with either treatment. When the wild-type is exposed to UV-B, gene expression is altered, therefore growth is altered. When the insertion mutants

were exposed to UV-B, gene expression and growth were not altered, due to the candidate gene not being present.

With insertion mutants, due to the deficiency of the assumed UV-B responsive photoreceptor, growth should not be altered with the Mylar or cellulose diacetate treatment. *ULI3* mutants also exhibited no phenotypic change relative to wild-type with respect to size, leaf-shape, and flowering time (Suesslin and Frohnmeyer, 2003). In the wild-type, UV-B alters the assumed photoreceptor, therefore altering gene expression, which results in altered growth.

The mutants with either treatment appear to have similar growth response to the wild-types with the cellulose diacetate treatment. The mutant growth is more than the wild-types with the Mylar treatment. It is possible that the insertion mutants may compensate for no UV-B by having less *COP1* activity (Oravecz et. al., 2006). When plants were exposed to blue light, *COP1* expression decreased, which resulted in increased growth (Oravecz et. al., 2006). When exposed to UV-B, *COP1* expression increased, which resulted in increased growth. Exposure to a combination of both, UV-B and blue light, will result in differential growth. If UV-B increased *COP1* expression by a factor and blue light decreases *COP1* expression by a factor, the results will be the average of growth between the two factors, or intermediate growth.

My hypothesis predicted that there would be increased growth in the wild-type when exposed to the cellulose diacetate treatment when compared to the Mylar treatment. Therefore, the similar or equal growth in the mutant when compared to the wild-type with the cellulose diacetate treatment may be due to changes in *COP1* activity. Wild-type plants with the Mylar treatment had less growth in comparison to the cellulose diacetate

treatment. This could be due to variable UV-B and blue light ratios. The Mylar treatment does not allow UV-B to pass through; therefore the plants were exposed to blue light. The blue light may have decreased *COP1* expression, which would result in increased growth. To test this possibility, the activity of *COP1* would be measured in the insertion mutants. A comparison of *COP1* levels in the wild-type would also be helpful information. It may also be of interest to create insertion mutants multi-deficient in *COP1,* other blue light responsive genes and our candidate gene receptor.

These data suggest that the candidate gene fits the proposed phenotype as a UV-B photoreceptor. Due to some inconsistent gene expression results, further studies are needed. In future work, using a larger data set by testing more genes that are known to be UV-affected will increase consistent results with gene expression. This will assist in the ability to resolve the role of the At2g02710. Comparing the effects of UV-B from the lab setting to *Arabidopsis* original geographic location may also help to identify if the plants have higher tolerance to UV-B. It is possible that its genes have the ability to become tolerable to various levels of UV-B; therefore thirty minutes of UV-B may not have much effect. To fully assess fitness, I would monitor growth along with other growth factors such as seed production, seed weight, and seed size. I would also increase the sample size for more consistent growth effect results.

LITERATURE CITED

Ahmad, M. and Cashmore, A. (1993). HY4 gene of *Arabidopsis thaliana* encodes a protein with characteristics of a blue-light photoreceptor. Nature. 366:162-166.

Boccalandro, H.E., Mazza, C.A., Mazzella, M.A., Casal, J.J., and Ballare, C.L. (2001). Ultraviolet B radiation enhances a phytochrome-b-mediated photomorphogenic response in *Arabidopsis*. Plant Phys. 126:780-788.

Briggs, WR. And Olney, MA. (2001) Photoreceptors in plant photomorphogenesis to date. Five phytochromes, two cryptochromes, one phototropin, and one superchrome. Plant Phys. 125:85-88.

Brown, B.A., Cloix, C., Jiang, G.H., Kaiserli, E., Herzyk, P., Kliebenstein, D.J., and Jenkins, G.I. (2005). A UV-B-specific signaling component orchestrates plant UV protection. PNAS. 102:18225-18230.

Catlett, NL., Yoder, OC., and Turgeon, BG. (2003). Whole-genome analysis of two-component signal transduction genes in fungal pathogens. E.C. 2:1151-1161.

Chen, M., Chory, J., and Fankhauser, C. (2004). Light signal transduction in higher plants. Annu. Rev. Genet. 38:87-117.

Christie, J. and Jenkins, G. (1996). Distinct UV-B and UV-A/blue light signal transduction pathways induce chalcone synthase gene expression in *Arabidopsis* cells. Plant Cell. 8:1555-1567.

DeBlasio, SL., Luesse, DL., and Hangarter, RP. (2005). A plant-specific protein essential for blue-light-induced chloroplast movements. Plant Phys. 139:101-114.

Frohnmeyer, H. and Staiger, D. (2003). Ultraviolet-B radiation-mediated responses in plants. Balancing damage and protection. Plant Phys. 133:1420-1428.

Ganeteg, U., Klimmek, F., and Jasson, S. (2004). Lhc5:an LHC-type protein associated with photosystem I. Plant Mol. Biol. 54:641-651.

Girke, T., Todd, J., Ruuska, S., White, J., Benning, C., and Ohlrogge, J. (2000). Microarray analysis of developing *Arabidopsis* seeds. Plant Phys. 124:1570-1581.

Green, R., and R. Fluhr. (1995). UV-B induced PR-1 accumulation is mediated by active oxygen species. Plant Cell. 7:203-212.

Hashimoto, T. 1994. Requirements of blue, UV-A, and UV-B light for normal growth of higher plants, as assessed by action spectra for growth and related phenomena, p 143-157. In: T.W.Tibbitts (ed.). International Lighting in Controlled Environments Workshop, NASA-CP-95-3309.

Hectors, K., Prinsen, E., Coen, W.D., Jansen, M.A.K., and Guisez, Y. (2007). *Arabidopsis thaliana* plants acclimated to low dose rates of ultraviolet B radiation

show specific changes in morphology and gene expression in the absence of stress symptoms. New Phytologist. 175(2):255-270.

Kim, B.C., Tenessen, D., and Last, R. (1998). UV-B induced photomorphogenesis in *Arabidopsis thaliana*. Plant J. 15:667-674.

Landry, L., Chapple, C., and Last, R. (1995). *Arabidopsis* mutants lacking phenolic sunscreens exhibit enhanced ultraviolet-B injury and oxidative damage. Plant Physiol. 109:1159-1166.

Li, J., Ou-Lee, T., Raba, R., Amundson, R., and Last, R. (1993). *Arabidopsis* flavonoid mutants are hypersensitive to UV-B irradiation. Plant Cell. 5:171-179.

Lin, C. (2002). Blue light receptors and signal transduction. Plant Cell. 14:S207-S225.

A-H Mackerness, S., Surplus, S.L., Blake, P., John, C.F., Buchanan-Wollaston, V., Jordan, B.R., and Thomas, B. (1999). Ultraviolet-B-induced stress and changes in gene expression in *Arabidopsis thaliana*: Role of signaling pathways controlled by jasmonic acid, ethylene and reactive oxygen species. Plant Cell Environ. 22:1413-1423.

Morelli, G. and Ruberti, I. (2002). Light and shade in the photocontrol of *Arabidopsis* growth. Trends Plant Sci. 7:399-403.

Motulsky, H.J. Analyzing Data with GraphPad prism. 1999. GraphPad Software Inc., San Diego CA, www.graphpad.com.

NASC (The Nottingham *Arabidopsis* Stock Centre). http://arabidopsis.info/

Nagaraj, SH., Gasser, RB., and Ranganathan, S. (2007). A hitchhiker's guide to expressed sequence tag (EST) analysis. Briefings in Bioinformatics. 8:6-21.

Nagatani, A., Reed, J., and Chory, J. (1993). Isolation and initial characterization of *Arabidopsis* mutants that are deficient in phytochrome A. Plant Physiol. 102:269-277.

Oravecz, A., Baumann, A., Mate, Z., Brzezinska, A., Molinier, J., Oakeley, E.J., Adam, E., Schafer, E., Nagy, F., and Ulm, R. (2006). Constitutively photomorphogenic1 is required for the UV-B response in *Arabidopsis*. The Plant Cell. 18:1875-1990.

Osterlund, MT., Hardtke, CS., Wei, N., and Deng, XW. (2000). Targeted destabilization of HY5 during light-regulated development of *Arabidopsis*. Nature. 405:462-466.

Parker, K., T.I. Baskin, W.R. Briggs. 1989. Evidence for phytochrome-mediated phototropism in etiolated pea seedlings. Plant Physiol. 89:493-497.

Pfaffl, M.W., Horgan, G.W., and Dempfle, L. (2002). Relative expression software tool (REST©) for group-wise comparison and statistical analysis of relative expression results in real-time PCR. Nucleic Acids Res. 30:(9):e36.

Ponting, CP and Aravind, L. (1997). PAS: a multifunctional domain family comes to light. Curr. Biol. 7:R674-R677.

Quail, P.H. (2002). Photosensory perception and signaling in plant cells: New paradigms? Curr. Opin. Cell Biol. 14:**,** 180–188.

Reed, J., Nagpal, P., Poole, D., Furuya, M., and Chory, J. (1993). Mutations in the gene for the red-far-red light receptor phytochrome B alter cell elongation and physiological responses throughout *Arabidopsis* development. Plant Cell. 5:147-157.

Schenk, P.M., Wilson, I., Anderson, J.P., Richmond, T., Somerville, S.C., and Manners, J.M. (2000). Coordinated plant defense responses in *Arabidopsis* revealed by microarray analysis. Proc. Natl. Acad. Sci. USA. 97:11655-11660.

Smith, H. (2000). Phytochromes and light signal perception by plants-An emerging synthesis. Nature. 407:585-591.

Somers, D.E., Sharrock, R.A., Tepperman, J.M., and Quail, P.H. (1991). The hy3 long hypocotyl mutant of *Arabidopsis* is deficient in phytochrome B. Plant Cell. 3:1263-1274.

Stapleton, A. (2006). NSF grant proposal.

Stapleton, A. (2006). RNA extraction protocol.

Suesslin, C. and Frohnmeyer, H. (2003). An *Arabidopsis* mutant defective in UV-B light mediated responses. The Plant Journal. 33:591-601.

Surplus, S.L., Jordan, B.R., Murphy, A.M., Carr, J.P., Thomas, B., and A-H Mackerness, S. (1998) Ultraviolet-B-induced responses in *Arabidopsis thaliana*: role of salicylic acid and reactive oxygen species in the regulation of transcripts encoding photosynthetic and acidic pathogenesis-related proteins. Plant, Cell and Environment. 21:685-694.

Taiz, L. and E. Zeiger. Plant Physiology 2nd Edition. Sinauer Associations. Massachusetts.1998.

Taylor, BL and Zhulin, IB. (1999). PAS domains: internal sensors of oxygen , redox potential, and light. Microbiol. Mol. Biol. Rev. 63:479-506.

The *Arabidopsis* Genome Initiative. 2000. Analysis sequence of the flowering plant *Arabidopsis thaliana*. Nature. 408:796-815.

Traw, M.B., Kniskern, J.M., and Bergelson, J. (2007). SAR increases fitness of *Arabidopsis thaliana* in the presence of natural bacterial pathogens. Evolution Int. J. Org. Evolution. 61:2444-2449.

Ulm, R., Baumann, A., Oravecz, A., Mate, Z., Adam, E., Oakeley, E.J., Schafer, E., and Nagy, F. (2004). Genome-wide analysis of gene expression reveals function of the bZIP transcription factor hy5 in the UV-B response of *Arabidopsis*. PNAS. 101:1397-1402.

Ulm, R. and Nagy, F. (2005). Signaling and gene regulation in response to ultraviolet light. Curr.Opin.Plant.Biol. 8:477-482.

UNEP, Environmental effects of ozone depletion: 1998 Assessment, United Nations environment programme, 205pp, 1998. ISBN 92-807-1724-3.

Wang, H. and Deng, X.W. (2002). Phytochrome signaling mechanism. In The *Arabidopsis* Book, C.R. Somerville and E.M. Meyerowitz, eds (Rockville, MD: American Society of Plant Biologists), doi/10.1199/tab.0074, http://www.aspb.org/publications/arabidopsis/.

Weigel, D. and Glazebrook, J. *Arabidopsis*: A Laboratory Manual. New York. Cold Spring Harbor Laboratory Press. 2002.

TABLES AND FIGURES

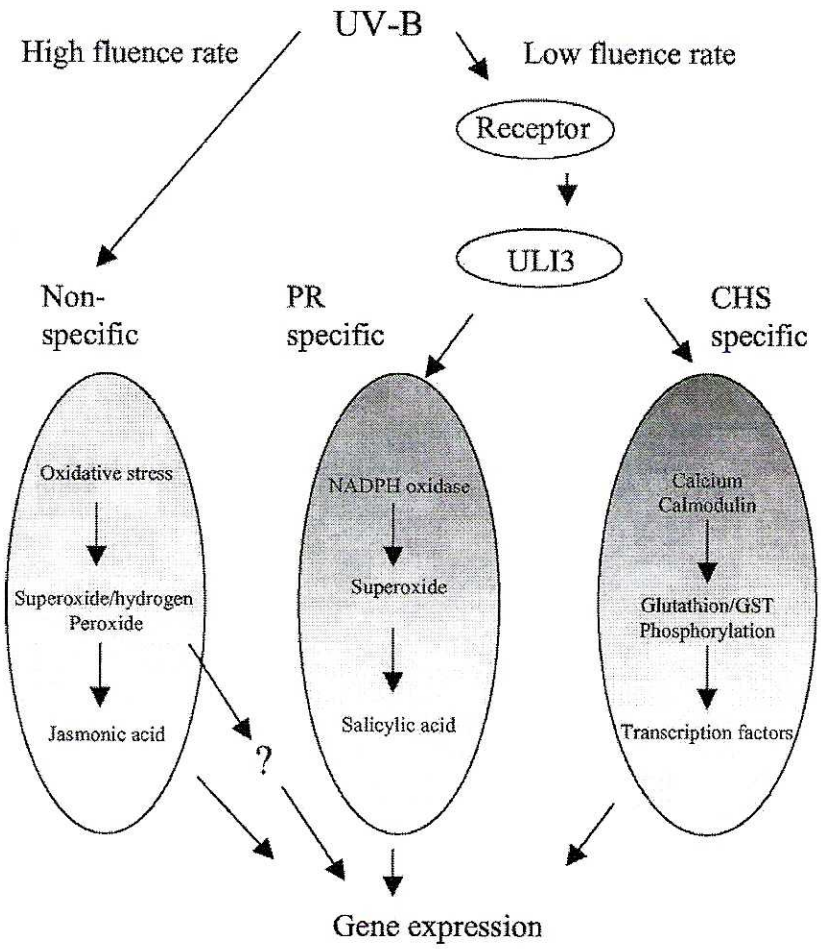

Fig. 1: Proposed model for UV-B-mediated signal transduction. The model is modified from Brosché and Strid (2003). PR, Pathogenesis-related protein; GST, glutathione *S*-transferase; ULI3, protein isolated from a UV-light-insensitive *Arabidopsis* mutant.

Table 1: The gene names and their left and right primer sequences. http://www.arabidopsis.org/portals/education/aboutarabidopsis.jsp.

Gene Name	Left Primer Sequence	Right Primer Sequence
Actin- Family protein produced/found in all cells.	AtactinL: 5'- TCC GTT TTG AAT CTT CCT CAA- 3'	AtactinR: 5'- CCG GTA CCA TTG TCA CAC AC - 3'
Hy5-Encodes a basic leucine zipper (bZIP) transcription factor that positively regulates photomorphogenesis.	Athy5qleft: 5'- ATC AAG CAG CGA GAG GTC AT- 3'	Athy5qright: 5'- AGC ATC TGG TTC TCG TTC TGA -3'
At5g59820- Encodes a zinc finger protein involved in high light and cold acclimation.	At59820qleft: 5'- GAC GCT TTG TCG TCT GGA TT -3'	At5g59820qr: 5'- GTG TCC TCC CAA AGC TTG TC -3'
At5g18470- Curculin-like (mannose-binding) lectin family protein	At5g18470qleft: 5'- GGA ACT TTG TGG TCC GAG AG -3'	At5g18470qr: 5'- CCC GGG AAG TAA TGT GTT TG -3'
At4g15480- Encodes a	At4g15480for: 5'- GGG	At4g15480rev: 5'- TCG

protein that might have sinapic acid:UDP-glucose glucosyltransferase activity.	TGA TTA GAC CTC CAC CA-3’	AGT TCC ATC CAC AAT GA -3’
At3g25250- *Arabidopsis* protein kinase.	At3g25250qleft: 5’- TGT TTT CCG ACG AGA TTA TCA -3’	At3g25250qr: 5’- TCT GGC TTC AAA TCT CTA TAC ACA -3’
At2g38940- phosphate transporter (AtPT2).	At2g38940for: 5’- CAC AAA AGC CTG GGA CTC TC-3’	At2g38940rev: 5’- TGG TTG CGG ATA AAG GGT AG-3’
At2g32020- GCN5-related N-acetyltransferase (GNAT) family protein	At2g32020qleft: 5’- TTG GGC CAC AGA TCC TAA AG -3’	At2g32020qr: 5’- GGA CGG TCG TCT TCT AAG CA -3’

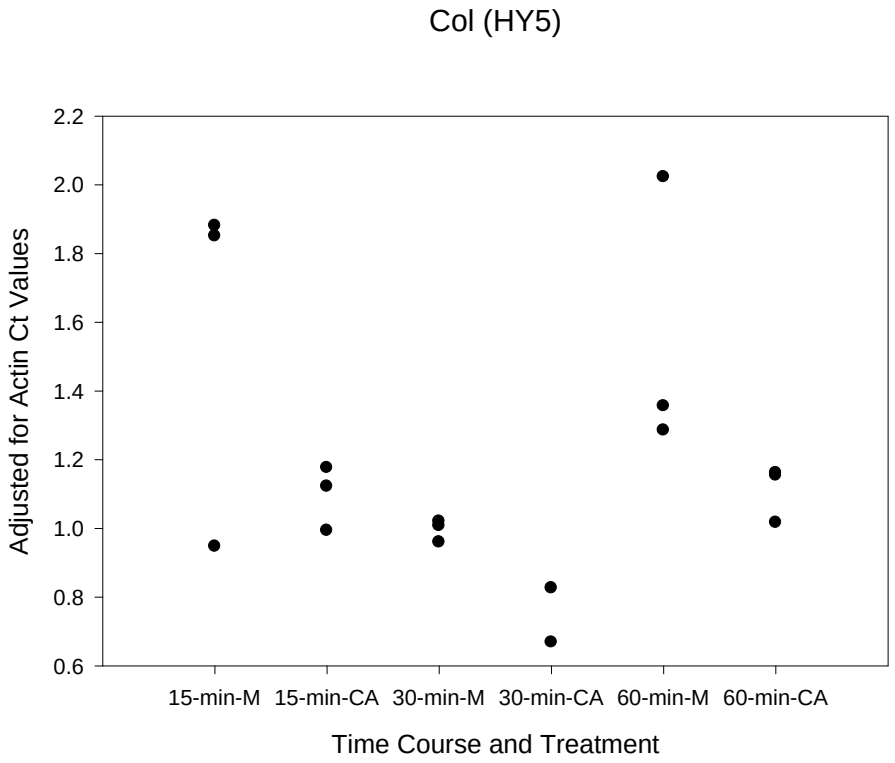

Figure 2: Measurement of gene expression with increasing UV-B levels in Columbia wild-type plants. The treatments used were Mylar, which was used as a control, and cellulose diacetate (CA), which allowed UV-B to pass through. Transcript levels for this gene were measured by real-time-PCR (RT-PCR) and actin was used as a control. The points displayed are the cycle threshold (Ct) values, which were output from RT-PCR. The Ct values from the HY5 primers were divided by the Ct value from the actin primers for each sample to get the adjusted for actin Ct values. Each point represents one replicate (n=2-3).

Table 2: Relative Expression Software Tool (REST) output, which was a pairwise comparison of gene expression. The treatments were Mylar, which was used as a control, and cellulose diacetate, which allows UV-B to pass through. The wild-type genotypes used were Col, 600C, and 6Fsx. The mutant genotypes used were 600I, 6F, and 600A. Initially, seven known UV-affected genes were used, but due to unreliability, HY5 was only used in Col, 600I and 6F genotypes. The rows highlighted in yellow represent the genes that were consistently regulated by UV-B. The rows highlighted in red represent the gene that consistently exhibited differential responses to UV-B treatment. These numbers represent the amount by which each gene is up- or down-regulated by UV-B plus/minus the standard error.

Wild-Type			**Mutant**		
Line	Gene	Adjusted by +UV/-UV Comparison	Line	Gene	Adjusted by +UV/-UV Comparison
Col	HY5	DOWN-regulated by -5.661±0.503	**600I**	HY5	DOWN-regulated by -221.782±0.024
	At5g59820	UP-regulated by +7.235±10.597		At5g59820	UP-regulated by +267.983±765.092
	At5g18470	DOWN-regulated by -1.178±0.720		At5g18470	DOWN-regulated by -1.682±1.397
	At4g15480	UP-regulated by +31.713±107.656		At4g15480	UP-regulated by +3.740±3.020
	At3g25250	UP-regulated by +9.158±13.709		At3g25250	DOWN-regulated by -1.027±2.347
	At2g38940	UP-regulated by +6.485±14.210		At2g38940	DOWN-regulated by -1.240±0.604
	At2g32020	UP-regulated by +1.840±1.604		At2g32020	UP-regulated by +88.770±146.042
600C			**6F**	HY5	DOWN-regulated by -13.997±0.451
	At5g59820	DOWN-regulated by -15.032±0.197		At5g59820	UP-regulated by +4.708±8.00099
	At5g18470	DOWN-regulated by -4.033±1.229		At5g18470	DOWN-regulated by -26.373±0.098
	At4g15480	UP-regulated by +27.569±55.929		At4g15480	UP-regulated by +4.036±6.569
	At3g25250	UP-regulated by +1.004±4.585		At3g25250	DOWN-regulated by -1.132±4.058
	At2g38940	DOWN-regulated by -12.084±0.182		At2g38940	DOWN-regulated by -1.821±0.905
	At2g32020	UP-regulated by +1.245±1.984		At2g32020	DOWN-regulated by -1.376±1.229
6Fsx			**600A**		
	At5g59820	UP-regulated by +135.956±373.331		At5g59820	DOWN-regulated by -216.617±0.012
	At5g18470	UP-regulated by +187.663±496.072		At5g18470	DOWN-regulated by -5.162±0.280
	At4g15480	UP-regulated by +1.199±1.230		At4g15480	DOWN-regulated by -5.344±0.226
	At3g25250	UP-regulated by +37.143±120.841		At3g25250	DOWN-regulated by -1.371±1.241
	At2g38940	DOWN-regulated by -2.360±0.401		At2g38940	DOWN-regulated by -15.412±0.068
	At2g32020	UP-regulated by +192.405±603.515		At2g32020	DOWN-regulated by -139.779±0.019

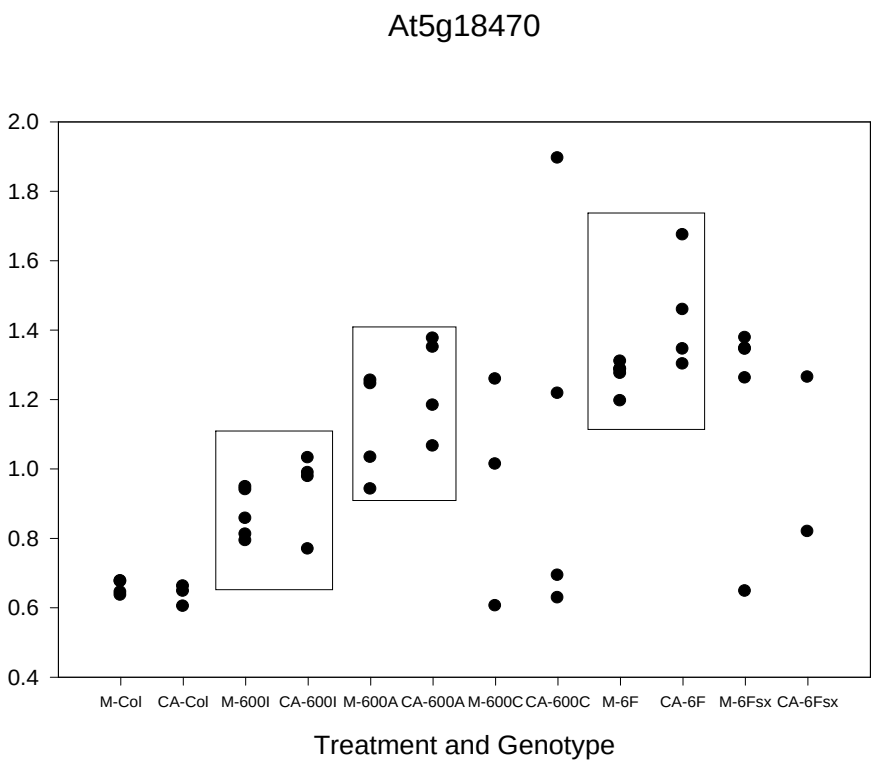

Figure 3: Gene At5g18470 expression was measured by RT-PCR and actin was used as a control. The treatments used were Mylar, which was used as a control, and cellulose diacetate (CA), which allowed UV-B to pass through. The points displayed are the cycle threshold (Ct) values, which were output from RT-PCR. The Ct values from the At5g18470 primers were divided by the Ct value from the actin primers for each sample to get the adjusted for actin Ct values. The wild-type genotypes used were Col, 6Fsx, and 600C. The mutant genotypes used were 600I, 600A, and 6F. The boxes are plotted to categorize the mutant genotypes for easier comparison. This shows the effects of UV-B on gene expression in mutant and wild-type genotypes under UV-B. Each point represents one replicate (n=2-6).

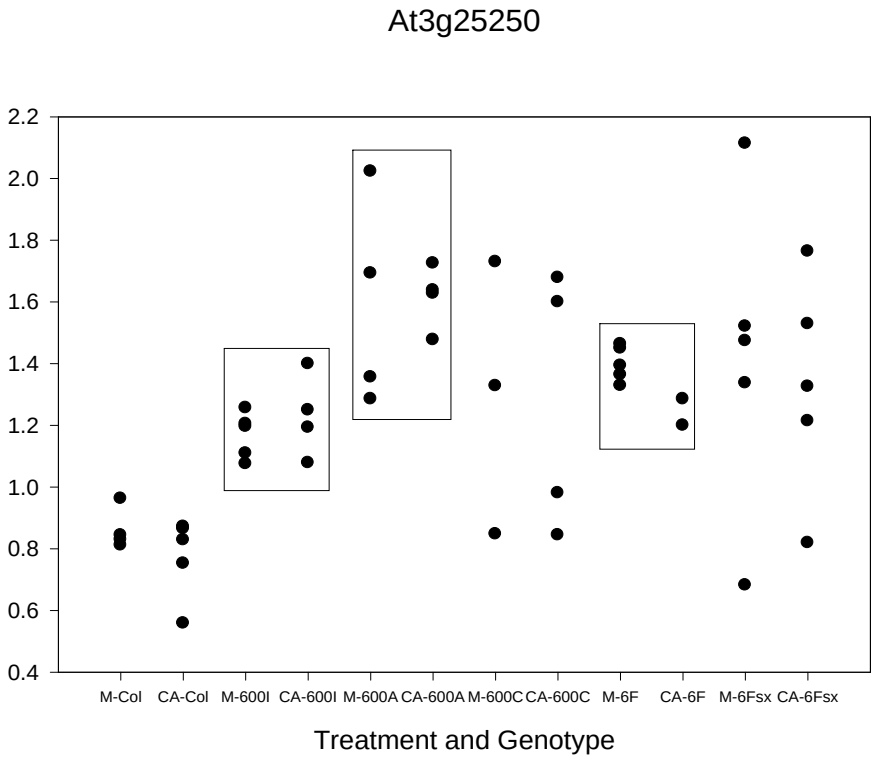

Figure 4: Gene At3g25250 expression was measured by RT-PCR and actin was used as a control. The treatments used were Mylar, which was used as a control, and cellulose diacetate (CA), which allowed UV-B to pass through. The points displayed are the cycle threshold (Ct) values, which were output from RT-PCR. The Ct values from the At5g18470 primers were divided by the Ct value from the actin primers for each sample to get the adjusted for actin Ct values. The wild-type genotypes used were Col, 6Fsx, and 600C. The mutant genotypes used were 600I, 600A, and 6F. The boxes are plotted to categorize the mutant genotypes for easier comparison. This shows the effects of UV-B on gene expression in mutant and wild-type genotypes under UV-B. Each point represents one replicate (n=6).

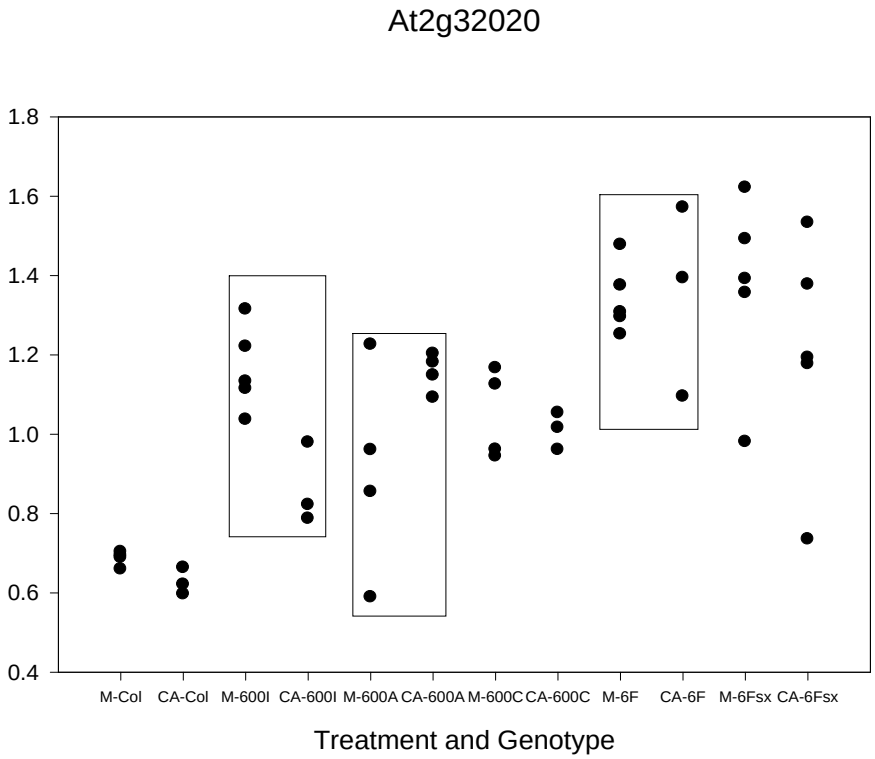

Figure 5: Gene At2g32020 expression was measured by RT-PCR and actin was used as a control. The treatments used were Mylar, which was used as a control, and cellulose diacetate (CA), which allowed UV-B to pass through. The points displayed are the cycle threshold (Ct) values, which were output from RT-PCR. The Ct values from the At5g18470 primers were divided by the Ct value from the actin primers for each sample to get the adjusted for actin Ct values. The wild-type genotypes used were Col, 6Fsx, and 600C. The mutant genotypes used were 600I, 600A, and 6F. The boxes are plotted to categorize the mutant genotypes for easier comparison. This shows the effects of UV-B on gene expression in mutant and wild-type genotypes under UV-B. Each point represents one replicate (n=2-6).

Table 3: Bootstrap permutation testing was used to estimate the sampling distribution to compare each genotype, treatment level and their interaction. Seven genes were used and their transcript levels were measured by RT-PCR. The Ct values from each primer was divided by the Ct value from the actin primers for each sample to get the adjusted for actin Ct values. These numbers represent the calculated p-values from the bootstrap test, which tells whether there was a significant difference between their treatments (Mylar and CA), genotypes (mutant and wild-type), and their interaction (genotype and treatment).
*Significant.

	HY5	At5g59820	At5g18470	At4g15480	At3g25250	At2g38940	At2g32020
Genotype	0.432	0.993	1	0.998	1	1	1
Treatment	0.37	0.254	0.893	0.973	0.475	1	0.449
Interaction	0.423	0.254	0.31	0.75	0.046*	0.667	0.108

Table 4: ANOVA comparison from JMP statistical software. This table shows calculated p-values from actin-adjusted data, which indicated whether the actin-adjusted gene expression was significantly altered when genotypes were grouped into mutant (Mut) and wild-type (Wt) classes. The treatments used were Mylar, which was used as a control, and cellulose diacetate (CA), which allowed UV-B to pass through. The Mut/Wt*Treatment represents the interaction of the genotypes and the treatments. *Significant

Gene	Treatment	Mut/Wt	Mut/Wt*Treatment
At5g59820	0.7835	0.0228*	0.9123
At5g18470	0.3037	0.0021*	0.8000
At4g15480	0.0304*	0.2466	0.1824
At3g25250	0.7222	0.0007*	0.8569
At2g38940	0.3743	0.0543	0.8910
At2g32020	0.0488	<.0001*	0.9558

Table 5: Tukey's HSD test comparison of least-square means for actin-adjusted gene expression when genotypes were grouped into mutant (Mut) and wild-type (Wt) classes. Six known UV-affected genes were used. The Mut/Wt*Treatment represents the interaction of the genotypes and the treatments. Levels not connected by the same letter in a column are significantly different.

Gene	Treatment	Mut/Wt	Mut/Wt*Treatment
At5g59820	Mylar^{A}	Mutant^{A}	Mutant, Mylar^{A}
	CA^{A}	Wild-type^{B}	Mutant, CA^{A}
			Wild-type, Mylar^{A}
			Wild-type, CA^{A}
At5g18470	Mylar^{A}	Mutant^{A}	Mutant, Mylar$^{A\ B}$
	CA^{A}	Wild-type^{B}	Mutant, CA^{A}
			Wild-type, Mylar ^{B}
			Wild-type, CA$^{A\ B}$
At4g15480	Mylar^{A}	Mutant^{A}	Mutant, Mylar^{A}
	CA^{B}	Wild-type^{A}	Mutant, CA^{A}
			Wild-type, Mylar^{A}
			Wild-type, CA^{A}
At3g25250	Mylar^{A}	Mutant^{A}	Mutant, Mylar^{A}
	CA^{A}	Wild-type^{B}	Mutant, CA^{A}
			Wild-type, Mylar$^{A\ B}$
			Wild-type, CA^{B}
At2g38940	Mylar^{A}	Mutant^{A}	Mutant, Mylar^{A}
	CA^{A}	Wild-type^{B}	Mutant, CA^{A}
			Wild-type, Mylar^{A}
			Wild-type, CA^{A}
At2g32020	Mylar^{A}	Mutant^{A}	Mutant, Mylar^{A}
	CA^{A}	Wild-type^{B}	Mutant, CA^{A}
			Wild-type, Mylar ^{B}
			Wild-type, CA^{B}

Table 6: Comparison of actin-adjusted gene expression levels in mutants to a single wild-type, the Columbia line, using a Dunnett's test. How different the means are above the minimum significant difference is given as the absolute value of the means difference [Abs(Dif)] minus the least significant difference (Abs(Dif)-LSD); p-values of the two treatments are given, which indicates whether gene expression of the mutant genotypes was significantly different when compared to Col (wild-type) levels.
*Positive values show pairs of means that are significantly different.

	Mylar		**CA**	
Gene	Abs(Dif)-LSD	P-value	Abs(Dif)-LSD	P-Value
At5g59820	0.091*	0.0082	0.127*	0.0044
At5g18470	0.213*	0.0008	0.225*	0.0025
At4g15480	0.239*	0.0019	0.117*	0.0036
At3g25250	0.184*	0.0042	0.335*	0.0001
At2g38940	-0.13	0.5437	-0.09	0.3428
At2g32020	0.262*	0.0004	0.209*	0.0028

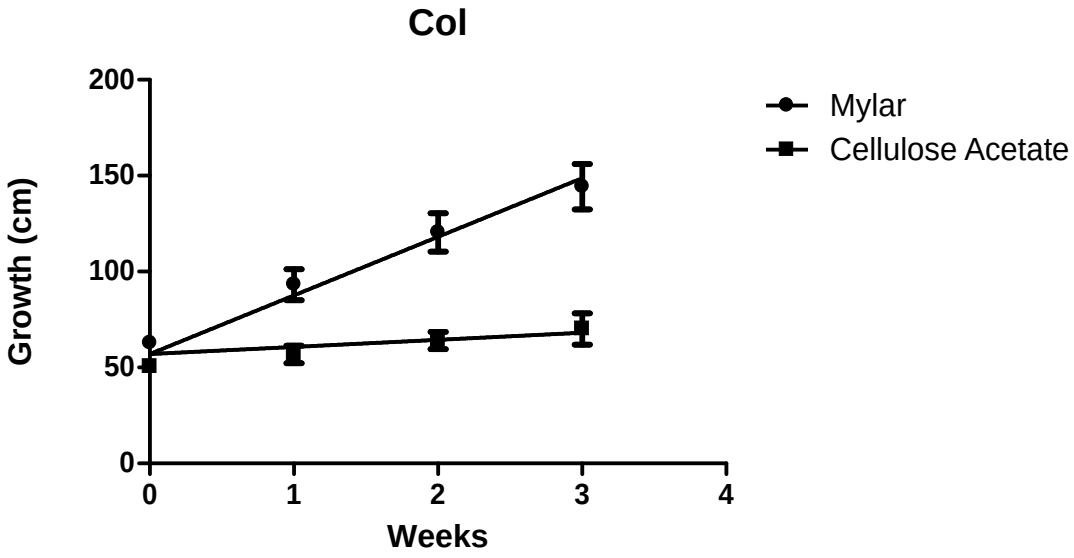

Figure 6: Linear regression of Columbia (wild-type) length of the rosette from tip to tip. The growth took place over a four-week time period in the lab setting under artificial lighting for each treatment. Error bars represent the standard error. (n=12)

Best-fit values	Mylar	Cellulose Diacetate
Slope	30.56 ± 2.342	3.719 ± 1.383
95% Confidence Intervals of Slope	25.79 to 35.33	0.7999 to 6.637

Table 7: The slopes and 95% confidence intervals of the growth linear regression for Columbia under artificial lighting for each treatment. The slope values are plus/minus the standard error. The 95% confidence interval values represent how well my data fit/defined the parameters, which was calculated from the standard error of the parameters. This table identifies whether slopes were significantly different between treatments and whether the lines were significantly different based on overlapping values.

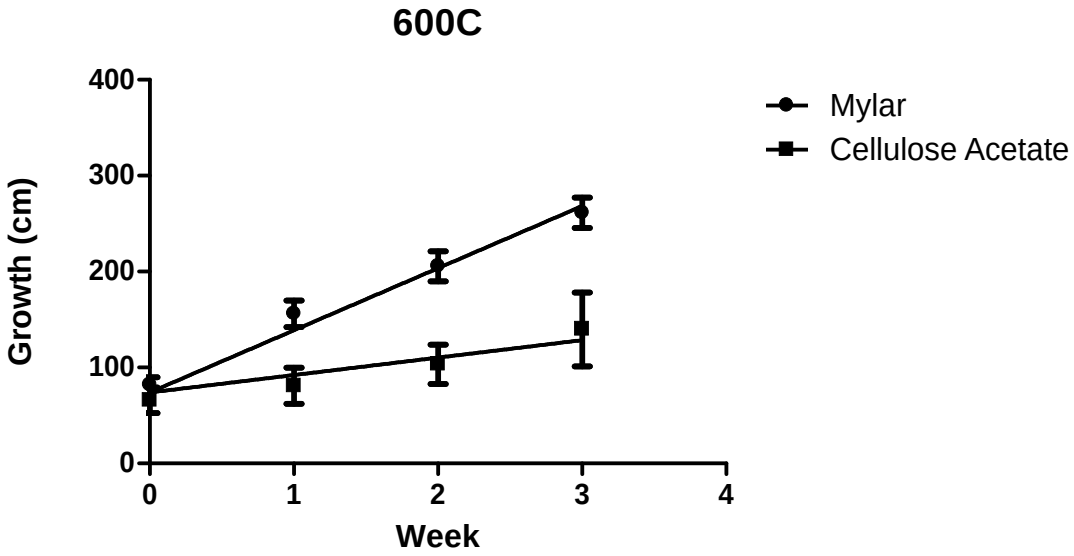

Figure 7: Linear regression of 600C (wild-type) length of the rosette from tip to tip. The growth took place over a four-week time period in the lab setting under artificial lighting for each treatment. Error bars represent the standard error. (n=12)

Best-fit values	Mylar	Cellulose Diacetate
Slope	64.77 ± 3.628	18.18 ± 5.732
95% Confidence Intervals Slope	57.43 to 72.11	5.886 to 30.48

Table 8: The slopes and 95% confidence intervals of the growth linear regression for 600C under artificial lighting for each treatment. The slope values are plus/minus the standard error. The 95% confidence interval values represent how well my data fit/defined the parameters, which was calculated from the standard error of the parameters. This table identifies whether slopes were significantly different between treatments and whether the lines were significantly different based on overlapping values.

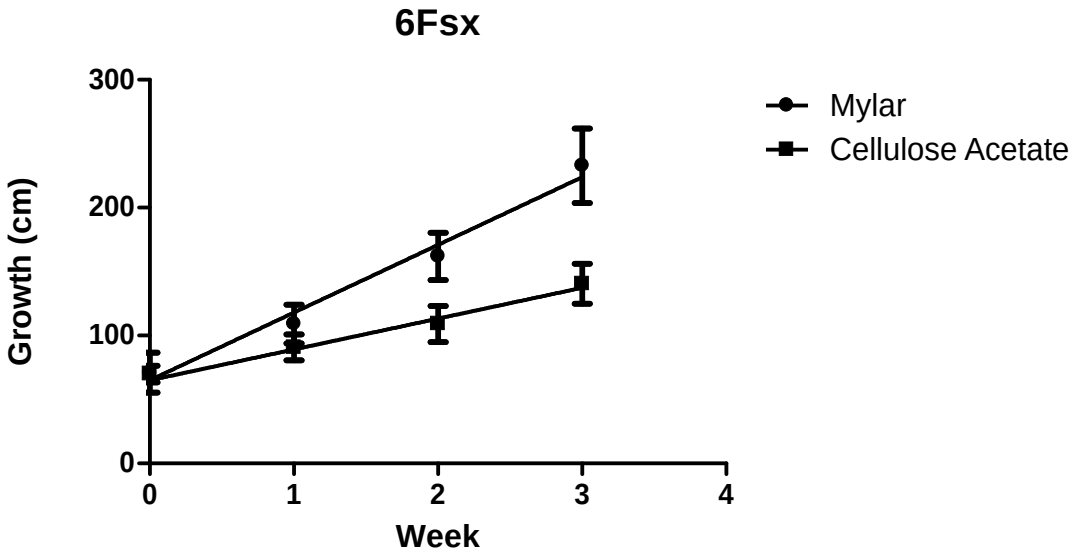

Figure 8: Linear regression of 6Fsx (wild-type) length of the rosette from tip to tip. The growth took place over a four-week time period in the lab setting under artificial lighting for each treatment. Error bars represent the standard error. (n=12)

Best-fit values	Mylar	Cellulose Diacetate
Slope	52.94 ± 5.098	24.12 ± 3.153
95% Confidence Intervals Slope	42.27 to 63.61	17.65 to 30.59

Table 9: The slopes and 95% confidence intervals of the growth linear regression for 6Fsx under the artificial light setting for each treatment. The slope values are plus/minus the standard error. The 95% confidence interval values represent how well my data fit/defined the parameters, which was calculated from the standard error of the parameters. This table identifies whether slopes were significantly different between treatments and whether the lines were significantly different based on overlapping values.

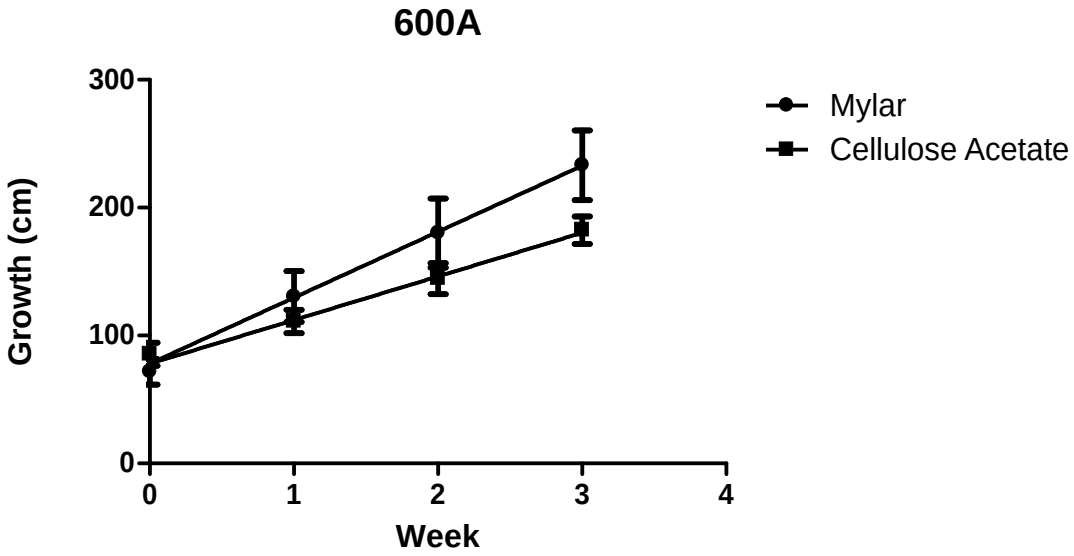

Figure 9: Linear regression of 600A (mutant) length of the rosette from tip to tip. The growth took place over a four-week time period in the lab setting under artificial lighting for each treatment. Error bars represent the standard error. (n=12)

Best-fit values	Mylar	Cellulose Diacetate
Slope	51.58 ± 5.690	34.12 ± 2.861
95% Confidence Intervals Slope	40.02 to 63.14	28.33 to 39.90

Table 10: The slopes and 95% confidence intervals of the growth linear regression for 600A under the artificial light setting for each treatment. The slope values are plus/minus the standard error. The 95% confidence interval values represent how well my data fit/defined the parameters, which was calculated from the standard error of the parameters. This table identifies whether slopes were significantly different between treatments and whether the lines were significantly different based on overlapping values.

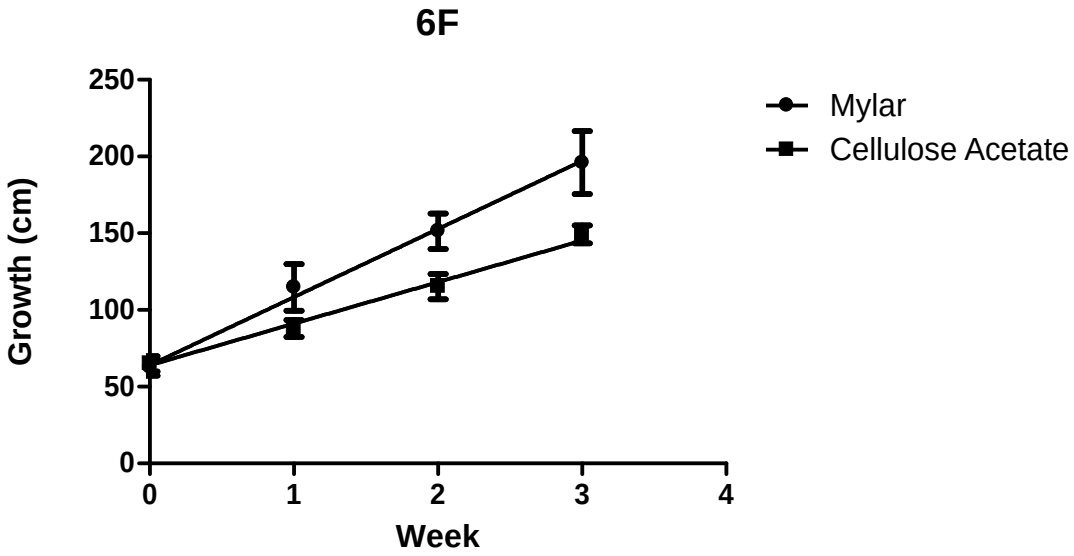

Figure 10: Linear regression of 6F (mutant) length of the rosette from tip to tip. The growth took place over a four-week time period in the lab setting under artificial lighting for each treatment. Error bars represent the standard error. (n=12)

Best-fit values	Mylar	Cellulose Diacetate
Slope	44.38 ± 3.639	27.07 ± 1.727
95% Confidence Intervals Slope	36.83 to 51.93	23.54 to 30.61

Table 11: The slopes and 95% confidence intervals of the growth linear regression for 6F under the artificial light setting for each treatment. The slope values are plus/minus the standard error. The 95% confidence interval values represent how well my data fit/defined the parameters, which was calculated from the standard error of the parameters. This table identifies whether slopes were significantly different between treatments and whether the lines were significantly different based on overlapping values.

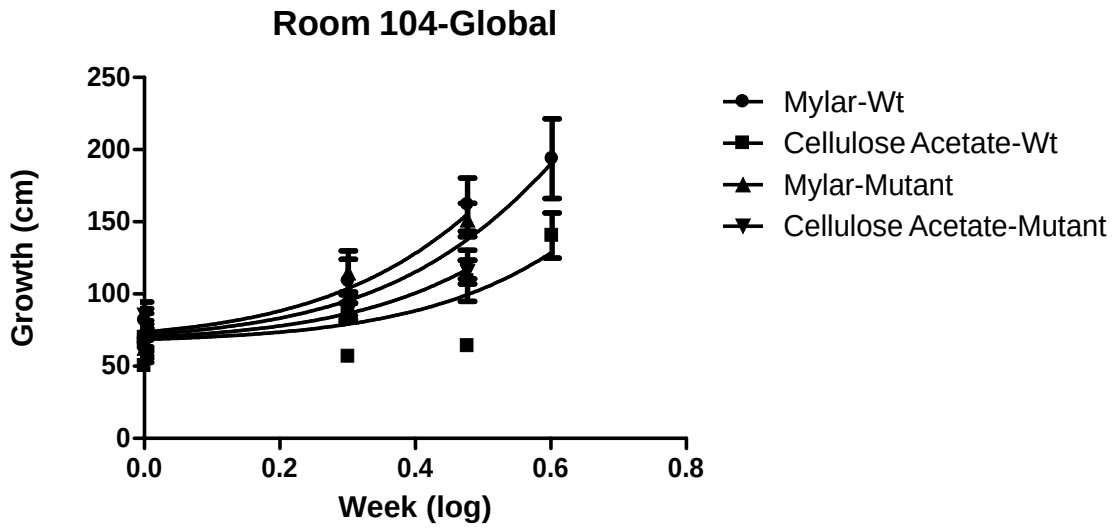

Figure 11: Global non-linear regression analysis of all rosette growth data from the lab setting under artificial lighting for each treatment. The mutants and the wild-types were grouped together. The group of wild-type (Wt) genotypes used were Col, 600C, and 6Fsx. The group of mutant genotypes used were 600A and 6F. Error bars represent the standard error. (n=12)

	Mylar-Wt	Cellulose Diacetate-Wt	Mylar-Mutant	Cellulose Diacetate-Mut
IC50	0.7786	0.9305	0.7315	0.8476
95% Confidence Interval	-0.7251 to 2.282	-0.5701 to 2.431	-0.7632 to 2.226	-0.6516 to 2.347

Table 12: Comparison of slopes for non-linear regression analysis of all growth data in the artificial light setting. Shared parameters and the curve mid-point (IC50) was calculated and examined for differences between the mutant and wild-type genotypes under each treatment condition. The 95% confidence interval values represent how well my data define the parameters.

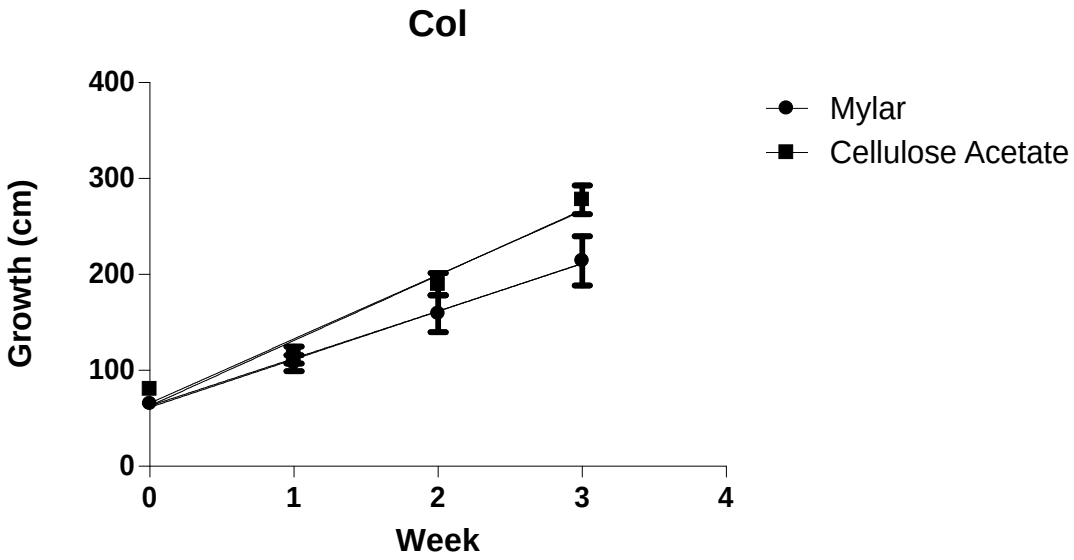

Figure 12: Linear regression of Columbia (wild-type) length of the rosette from tip to tip. The growth took place over a four-week time period in the UNCW greenhouse setting under artificial lighting for each treatment against the background daylight in the greenhouse. Error bars represent the standard error. (n=12)

Best-fit values	Mylar	Cellulose Diacetate
Slope	49.39 ± 4.524	68.04 ± 2.995
95% Confidence Intervals Slope	40.20 to 58.58	61.99 to 74.09

Table 13: The slopes and 95% confidence intervals of the growth linear regression for Columbia in the greenhouse. The slope values plus/minus the standard error. The 95% confidence interval values represent how well my data fit/defined the parameters, which were calculated from the standard error of the parameters. This table identifies whether slopes were significantly different between treatments and whether the lines were significantly different based on overlapping values.

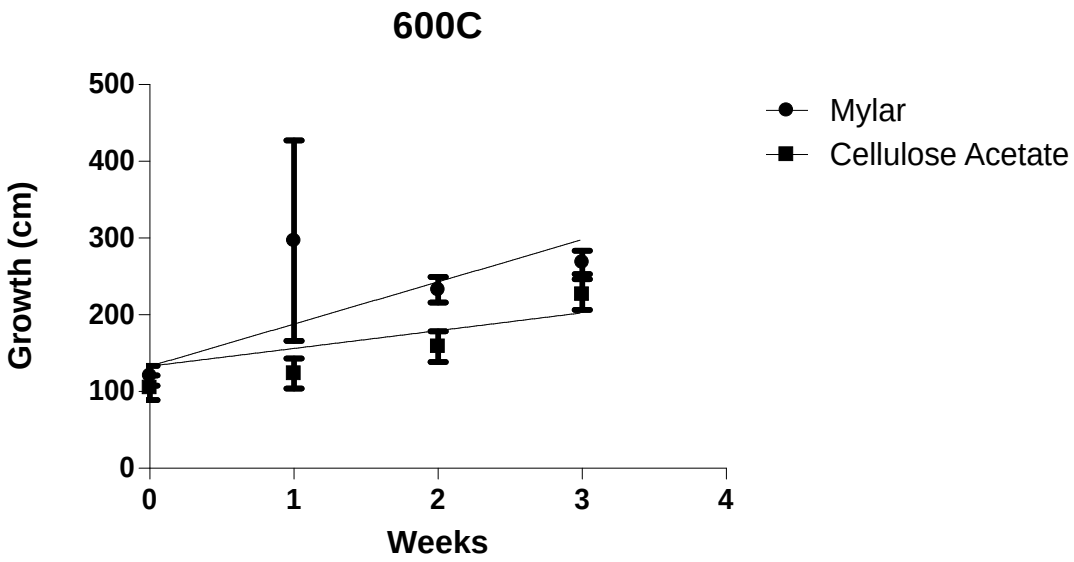

Figure 13: Linear regression of 600C (wild-type) length of the rosette from tip to tip. The growth took place over a four-week time period in the UNCW greenhouse setting under artificial lighting for each treatment against the background daylight in the greenhouse. Error bars represent the standard error. (n=12)

Best-fit values	Mylar	Cellulose Diacetate
Slope	54.97 ± 17.98	23.20 ± 5.278
95% Confidence Intervals Slope	18.68 to 91.26	12.48 to 33.92

Table 14: The slopes and 95% confidence intervals of the growth linear regression for 600C in the greenhouse. The slope values plus/minus the standard error. The 95% confidence interval values represent how well my data fit/defined the parameters, which were calculated from the standard error of the parameters. This table identifies whether slopes were significantly different between treatments and whether the lines were significantly different based on overlapping values.

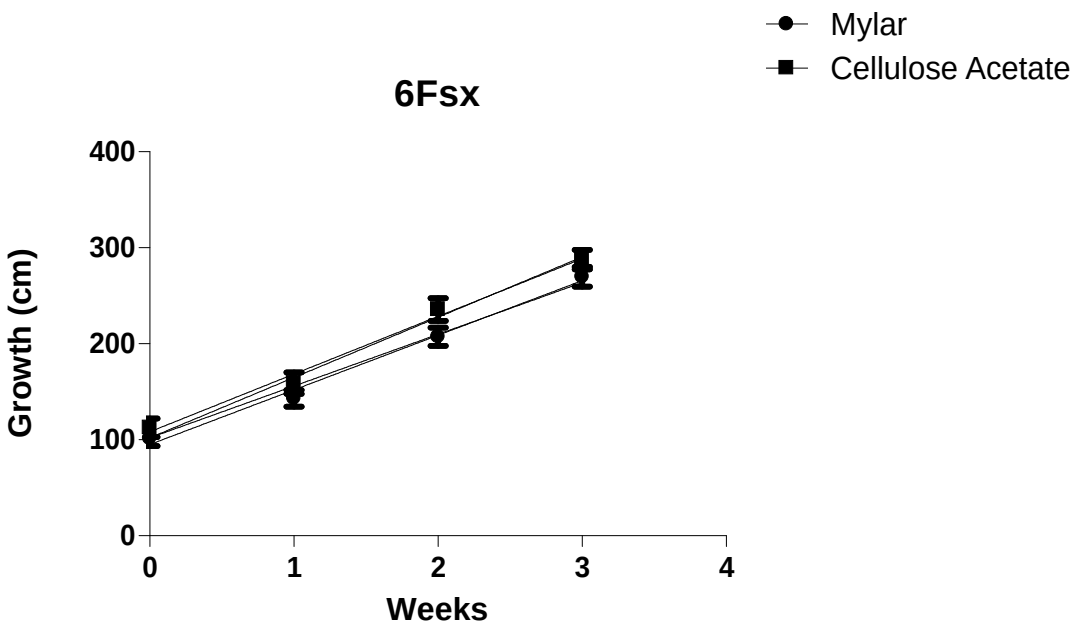

Figure 14: Linear regression of 6Fsx (wild-type) length of the rosette from tip to tip. The growth took place over a four-week time period in the UNCW greenhouse setting under artificial lighting for each treatment against the background daylight in the greenhouse. Error bars represent the standard error. (n=12)

Best-fit values	Mylar	Cellulose Diacetate
Slope	53.92 ± 2.425	62.80 ± 2.800
95% Confidence Intervals Slope	49.04 to 58.81	57.04 to 68.56

Table 15: The slopes and 95% confidence intervals of the growth linear regression for 600C in the greenhouse. The slope values plus/minus the standard error. The 95% confidence interval values represent how well my data fit/defined the parameters, which were calculated from the standard error of the parameters. This table identifies whether slopes were significantly different between treatments and whether the lines were significantly different based on overlapping values.

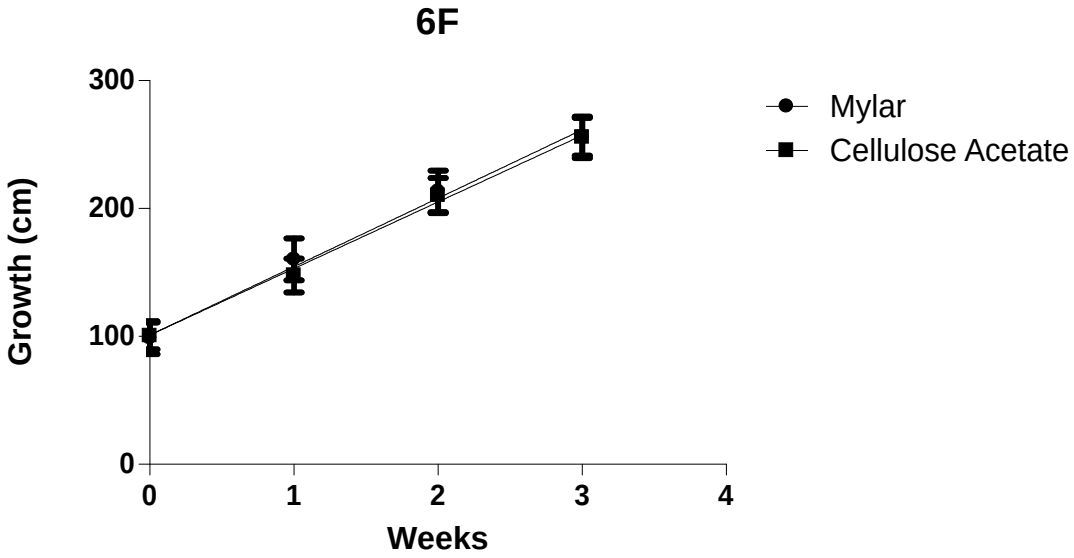

Figure 15: Linear regression of 6F (mutant) length of the rosette from tip to tip. The growth took place over a four-week time period in the UNCW greenhouse setting under artificial lighting for each treatment against the background daylight in the greenhouse. Error bars represent the standard error. (n=12)

Best-fit values	Mylar	Cellulose Diacetate
Slope	53.52 ± 3.870	52.05 ± 3.469
95% Confidence Intervals Slope	45.62 to 61.41	44.98 to 59.13

Table 16: The slopes and 95% confidence intervals of the growth linear regression for 6F in the greenhouse. The slope values plus/minus the standard error. The 95% confidence interval values represent how well my data fit/defined the parameters, which were calculated from the standard error of the parameters. This table identifies whether slopes were significantly different between treatments and whether the lines were significantly different based on overlapping values.

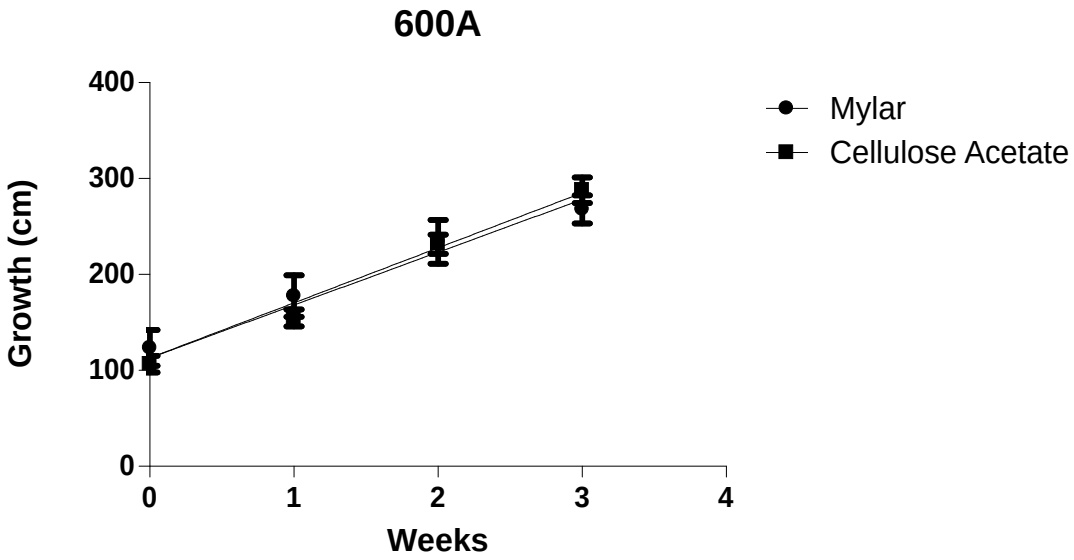

Figure 16: Linear regression of 600A (mutant) length of the rosette from tip to tip. The growth took place over a four-week time period in the UNCW greenhouse setting under artificial lighting for each treatment against the background daylight in the greenhouse. Error bars represent the standard error. (n=12)

Best-fit values	Mylar	Cellulose Diacetate
Slope	55.06 ± 5.089	57.34 ± 2.755
95% Confidence Intervals Slope	44.68 to 65.44	51.79 to 62.90

Table 17: The slopes and 95% confidence intervals of the growth linear regression for 600A in the greenhouse. The slope values plus/minus the standard error. The 95% confidence interval values represent how well my data fit/defined the parameters, which were calculated from the standard error of the parameters. This table identifies whether slopes were significantly different between treatments and whether the lines were significantly different based on overlapping values.

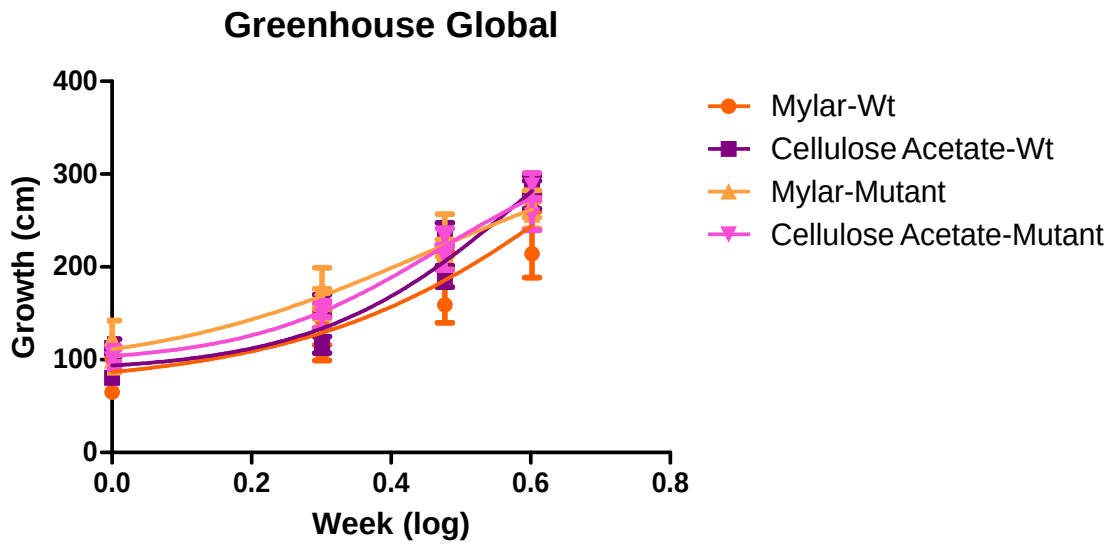

Figure 17: Global non-linear regression analysis of all rosette growth data from greenhouse growth setting. The mutants and the wild-types were grouped together. The group of wild-type (Wt) genotypes used were Col and 6Fsx. This data does not contain the wild-type, 600C, due to inability to characterize as mutant or wild-type based on growth pattern in the linear regression analysis. The group of mutant genotypes used were 600A and 6F. Error bars represent the standard error. (n=12)

	Mylar-Wt	Cellulose Diacetate-WT	Mylar-Mutant	Cellulose Diacetate-Mut
IC50	5.560	3.929	2.824	2.945
95% Confidence Intervals	-1.724 to 3.214	0.1019 to 1.087	-0.2115 to 1.113	0.2703 to 0.6677

Table 18: Comparison of slopes for non-linear regression analysis of all growth data in the greenhouse setting. Shared parameters and the curve mid-point (IC50) was calculated and examined for differences between the mutant and wild-type genotypes under each treatment condition. The 95% confidence interval values represent how well my data define the parameters.